

Supporting Information

Revealing Lectin-sugar Interactions with a Single Au@Ag Nanocube

Jingjing Shen^{a†}, Lei Zhang^{a†}, Li Liu^a, Bin Wang^a, Jieqiong Ba^a, Chao Shen^a, Yu Chen^a,
Quli Fan^{a*}, Shufen Chen^a, Weibing Wu^{b*}, Xiaomiao Feng^a, Lianhui Wang^a, Wei Huang^{ac*}*

^a Key Laboratory for Organic Electronics and Information Displays & Institute of Advanced Materials(IAM), National Synergistic Innovation Center for Advanced Materials (SICAM), Nanjing University of Posts & Telecommunications, 9 Wenyuan Road, Nanjing 210023, China

^b Jiangsu Provincial Key Lab of Pulp & Paper Science & Technology, Nanjing Forestry University, Nanjing, 210037, P.R. China.

^c Shaanxi Institute of Flexible Electronics (SIFE), Northwestern Polytechnical University (NPU), Xi'an 710072, China

E-mail: iamlzhang@njupt.edu.cn, wbwu@njfu.edu.cn, iamwhuang@njupt.edu.cn

Experimental Section

1. Materials and reagents

| Reagents / Drugs | Specifications | Source |
|---------------------------------|-----------------|------------|
| Chloroauric acid | 49%, Au basis | Sigma |
| Sodium borohydride | 98%, AR | Sigma |
| Ascorbic acid | 99%AR | Sigma |
| Cetyltrimethylammonium chloride | 96%, AR | BEHRINGING |
| Cetyltrimethylammonium bromide | 96%, AR | Sigma |
| Silver nitrate | 99% AR | Aladdin |
| Mannose (MW180.16) | 99% AR | Aladdin |
| Ethyl acetate | 99.5% AR | Aladdin |
| Petroleum ether | Spectral purity | Aladdin |

2. The Au nanocrystal seeds were prepared using a three-step procedure.

We first made 3 nm Au nanoparticles by adding 0.6 mL of ice-cooled NaBH_4 solution (10 mM) into a 10 mL aqueous solution containing HAuCl_4 (0.25 mM) and CTAB (100 mM), generating a brownish solution. The seed solution was kept undisturbed for 2 h at 28 °C to ensure complete decomposition of NaBH_4 remaining in the solution. For the synthesis of CTAC-capped Au seeds, 6 mL of aqueous HAuCl_4 solution (0.5 mM), 6 mL of aqueous CTAC solution (200 mM), and 3 mL of aqueous AA solution (100 mM) were mixed, followed by the addition of 0.3 mL of the 5 times diluted 3 nm Au nanoparticles. The mixture turned from colorless into red within 1 min, indicating the formation of 10 nm Au nanocrystals. 8 mL of aqueous HAuCl_4 solution (0.5 mM), 8 mL of aqueous CTAC solution (200 mM), and 3 mL of aqueous AA solution (100 mM) were mixed, followed by the addition of 1 mL of the 10 nm Au nanoparticles. The final mixture turned from colorless into red within 1 min, indicating the formation of 30 nm Au nanocrystals.

3. Synthesis of Au@Ag Nanocubes with Au Seeds in the Presence of CTAC.

In a typical procedure, 3 mL of the CTAC-Au seeds, 7 mL of CTAC (200 mM) aqueous solution and 3 mL aqueous solution of AA (100 mM) were mixed in a 20 mL vial. After the mixture was heated at 60 °C for 5 min under magnetic stirring, 0.6 mL aqueous AgNO₃ (10 mM) solution were injected at a rate of 0.2 mL/ 5 min using a syringe pump. During the injection, the reaction mixture turned from red to brownish-yellow. After 4 h, the vials were cooled in an ice-bath. The products were collected by centrifugation (5500 rpm for 5 min) and then washed with water once.

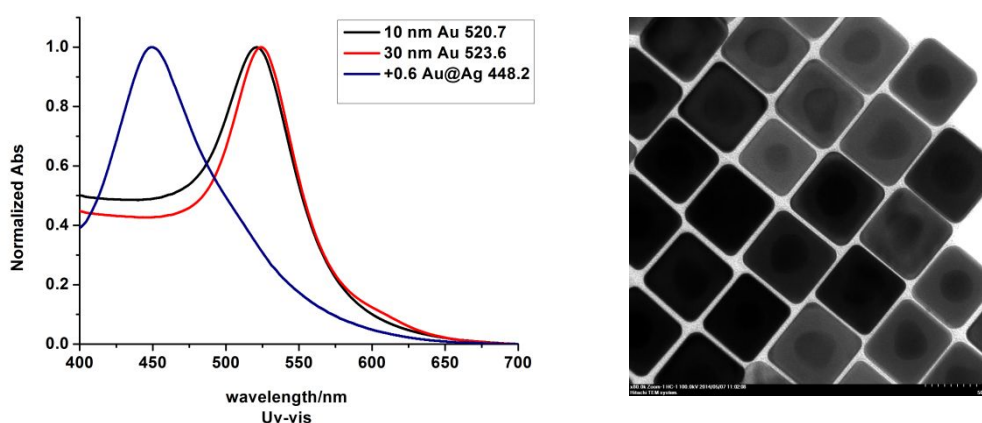


Figure S1. UV-vis extinction spectra of the process of Au@Ag NCs as labeled on the curve (left).

TEM images of Au@Ag NCs obtained by injecting 6 mL of AgNO₃ solution (10 mM).

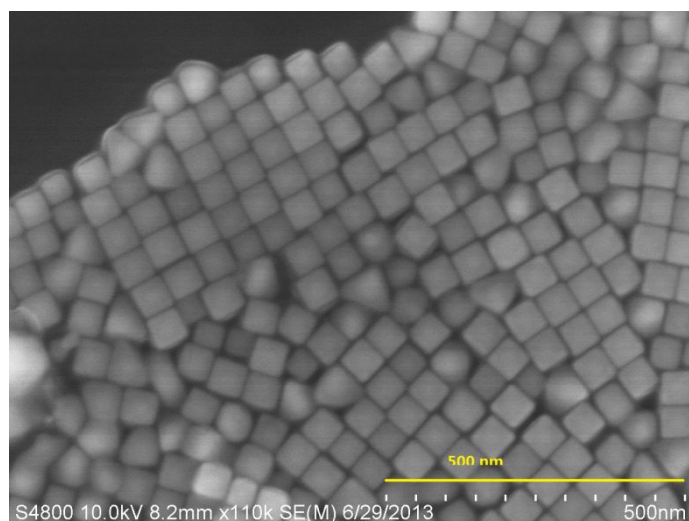


Figure S2. SEM images of Au@Ag NCs.

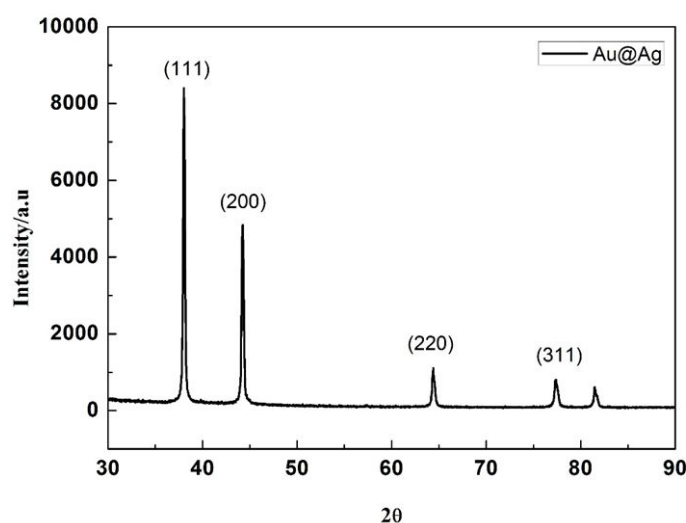


Figure S3. XRD spectrum of Au@Ag NCs.

4. Preparation of Au@Ag@Mannose probe

4.1 Immobilizations of the Au@Ag NCs onto the ITO glass substrate

The indium tin oxide (ITO) glasses were chosen as the sensing substrate for dark-field imaging and individual nanoparticle LSPR scattering measurements. ITO glass substrate was cleaned by ultrasonic cleaning in soapy water, acetone, ethanol, ultrapure water for at least 1h, respectively. After drying under N₂ beam, the ITO substrates were stored in clean centrifuge tube for next using. Au@Ag NCs could be immobilized on the glasses surface by physical absorptions effect. The processed ITO glass immersing into diluted nanoparticles solutions for 30s, then followed removing superfluous Au@Ag NCs by washing ultrapure water and drying it under a weak stream of N₂ gas.

4.2 Modification of thiolated D-mannose on Au@Ag NCs.

There had been many reports[1-3] about assembly of disulfide bond on gold or silver. Therefore, thiolated D-mannose was designed to be modified with a disulfide bond for the better combination with Au@Ag NCs. 200 μ L of 1 mM thiolated D-mannose solution was

pipetted onto the surface of the Au@Ag NCs modified ITO glass slide, and then incubated in the shaker with 30 rpm at room temperature for a certain time.

4.3 the number analysis of thiolated D-mannose

5. Equipmental instrument

The DFM images, SPR scattering spectroscopy measurements were recorded by an inverted microscope equipped with a monochromator (eclipse Ti-U, Nikon) (Acton SP2358), a -75 °C cooled CCD detector (PIXIS 400BR: excelon, Princeton Instruments) and a 532 nm continuous-wave laser light (Spectra-Physics Excelsior, 100 mW). The microscope was equipped with a 60× objective lens, a dark field condenser ($0.8 < \text{numerical aperture(NA)} < 0.95$), and a true-color digital camera (Nikon DS-f2). The spectra were integrated through a 1 μm slit width. All the measurements were performed at room temperature. The LSPR scattering signal light was splited when it passes through the grating of 300 G/mm with 500 nm blaze wavelength, and the optical signal is received by the spectrograph CCD with 1340 pixels in length. Spectral data with the wavelength width of 279 nm are collected at one time. The spectral data received by each pixel represents the resolution of the spectrometer, which is 279/1340 nm (0.208 nm).

UV-vis absorption spectra were obtained by a Shimadzu UV3600 spectrophotometer. Scanning electron microscope (SEM) images were collected with S-4800 instrument (Japan). Transmission electron microscope (TEM) images were taken on a JEM 2010 instrument (Japan). X-Ray Diffraction (XRD) patterns were acquired by Bruker D8 Advance diffractometer.

6. Analysis application of Au@Ag@Mannose probes

6.1 Detection of trace ConA with Au@Ag@Mannose probe

For analysis of trace ConA and interfering protein by LSPR scattering measurement, firstly, the functionalized ITO slide with Au@Ag@Mannose probe immobilized on its surface was put on the automatic stage, and then 100 μL of target oligonucleotide solution were pipetted on the surface of the ITO slide. The scattering spectra of the individual nanocubes were continually collected for 20 seconds and corrected by subtracting the background spectra and then divided with the calibrated response curve of the entire optical system.

6.2 control experiments for detection of ConA

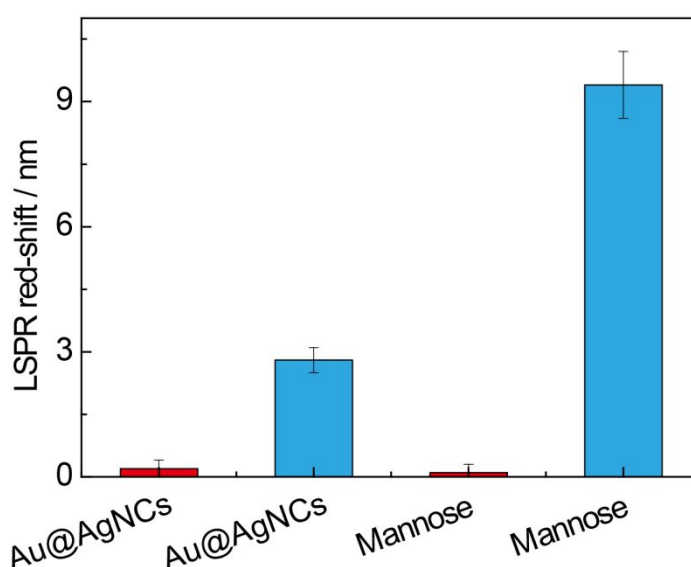


Figure S4. The LSPR scattering spectra red-shift degree after reaction for 120 min at different condition. From left to right: 1) Au@Ag NCs in water, 2) Au@Ag NCs in 0.1 μM ConA solution, 3) Au@Ag@Mannose in water, 4) Au@Ag@Mannose in 0.1 μM ConA solution.

Control experiments were employed to verify the plasmonic nanobiosensors are sensitive to ConA. Before and after treatment with water, the LSPR scattering spectra of Au@AgNCs and Au@Ag@Mannose probe remain its original position. With presence of 0.1 μM ConA, the Au@AgNCs showed a small shift to long wavelength about 2.9 nm. This result indicated

there was a small change in the RI around the nanoparticles which could contribute to the physical absorption effect between Au@AgNCs and ConA. For Au@Ag@Mannose, due to the specific binding ability between mannose and ConA, the LSPR scattering spectra red-shift notably up to 9.8 nm.

6.3 Control experiments in colloid solution of Au@Ag@Mannose

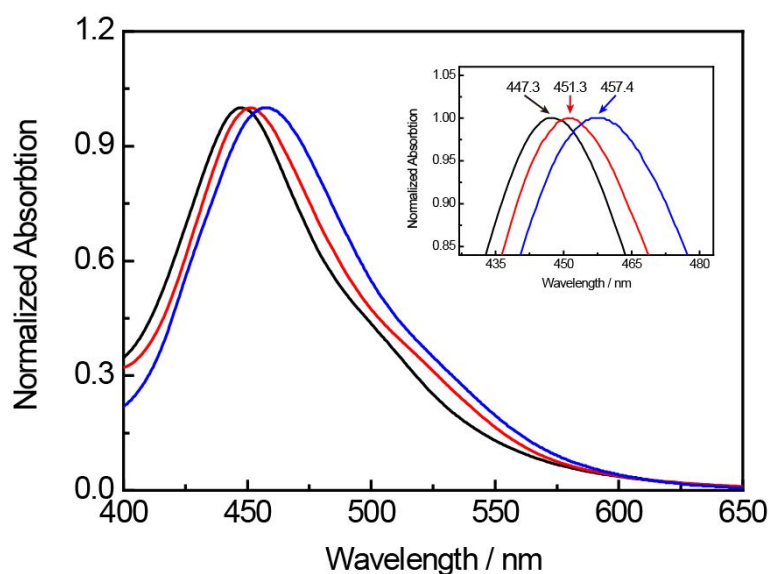


Figure S5. UV-vis spectra of colloidal solution of Au@Ag NCs (black), Au@Ag@Mannose (red) and Au@Ag@Mannose with specific binding of ConA (blue).

Figure S5 showed the normalized absorption spectra of colloid solution of original Au@Ag NCs (black), Au@Ag@Mannose probes (red), and the probe after incubation with 0.1 μ M ConA (blue). The peak of Au@Ag NCs located 447.3 nm. After modification by 1 mM thiolated D-mannose, the absorption spectra peak red-shifted to 451.3 nm which indicated that the successful modification of D-mannose and preparation of Au@Ag@Mannose probe. After ConA was specific bonded on the surface of Au@Ag@Mannose probe, the extinction spectra shifted further to 457.4 nm. All the peak position of extinction spectra

mentioned above were blue than the plasmonic nanoparticles on ITO (Indium Tin Oxide) glass, which could be contributed to the larger reflective index of the Indium Tin Oxide and SiO_2 . When Au@Ag NCs were immobilized on the ITO surface, the surrounding environment RI would increase greatly, and it would lead to the LSPR scattering spectra shift to longer wavelength. And this result had been verified in our previous report^[4-6].

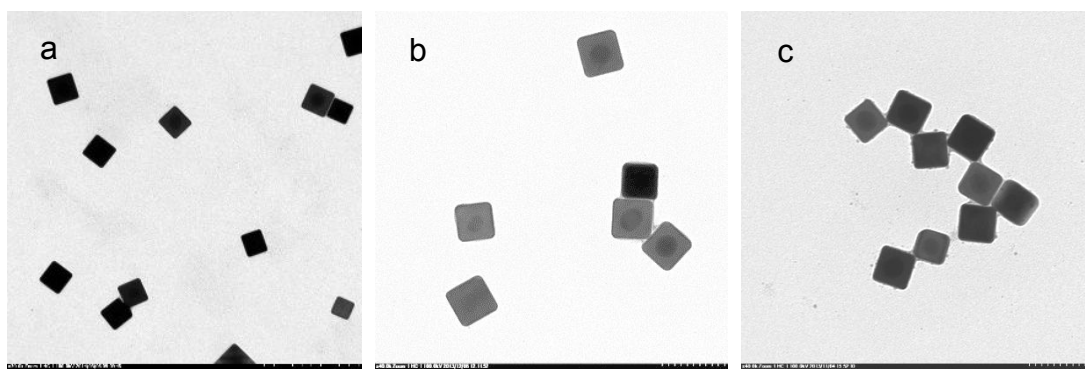


Figure S6. TEM images of colloid solution of Au@Ag NCs (a), Au@Ag@Mannose probe before (b) and after (c) incubated with $0.1 \mu\text{M}$ ConA.

The Au@Ag NCs were synthesized by seed-mediated growth method with about 55 nm. After modified by thiolated D-mannose and cleaning with plenty of deionized water, there was still a notable organic film on the Au@Ag NCs surface which indicated that the D-mannose was successfully immobilized on Au@Ag NCs surface, and this results could be proved by its extinction spectrum red-shift to long wavelength compared with original Au@Ag NCs. And the edge of Au@Ag NCs almost has only dinky change in the curve radius of tips before and after modified with thiolated D-mannose (From about 7 nm to 8 nm). After treatment with the certain concentration of ConA solution, there was no obviously change in the Au@Ag NCs shape and edge.

7. Organic synthesis

D-Mannose (2.50 g, 13.9 mM) was dissolved in pyridine dried with Na_2SO_4 (20 mL) and acetic anhydride (10 mL) added. After stirring for 16 h at r.t., the reaction mixture was concentrated in vacuum, the residue dissolved in ethyl acetate, washed successively with sat. NaHCO_3 (3×100 mL) and sat. NaCl (2×100 mL), and dried with Na_2SO_4 . Ethyl acetate was removed to yield peracetylated mannose (4.8 g, 89%, mixture of both anomers) as a clear viscous. ^1H NMR (400 MHz, CDCl_3 , mixture of both anomers): signals of β -anomer δ (ppm) = 2.00 (s, 3H, COCH_3), 2.04 (s, 3H, COCH_3), 2.09 (s, 3H, COCH_3), 2.16 (s, 3H, COCH_3), 2.21 (s, 3H, COCH_3), 3.99–4.05 (m, 1H, 5-H), 4.07 (dd, J = 2.4, 12.4 Hz, 1H, 6-Ha), 4.26 (dd, J = 4.9, 12.4 Hz, 1H, 6-Hb), 5.27 (dd, J = 2.0, 3.1 Hz, 1H, 3-H), 5.33–5.35 (m, 2H, 3-H, 4-H), 6.09 (d, J = 2.0 Hz, 1H, 1-H); signals of α -anomer δ (ppm) = 2.00 (s, 3H, COCH_3), 2.03 (s, 3H, COCH_3), 2.07 (s, 3H, COCH_3), 2.15 (s, 3H, COCH_3), 2.16 (s, 3H, COCH_3), 3.79 (m, J = 2.4, 5.3, 9.9 Hz, 1H, 5-H), 4.11 (dd, J = 2.4, 12.4 Hz, 1H, 6-Ha), 4.28 (dd, J = 5.3, 12.4 Hz, 1H, 6-Hb), 5.13 (dd, J = 3.3, 10.0 Hz, 1H, 3-H), 5.27 (t, J = 10.0 Hz, 1H, 4-H), 5.48 (dd, J = 1.2, 3.3 Hz, 1H, 2-H), 5.95 (d, J = 1.2 Hz, 1H, 1-H);

6.4 mL of $\text{BF}_3 \cdot \text{Et}_2\text{O}$ (7.2 g, 5 eq, 51.2 mM) was added dropwise to a solution of Bis(2-hydroxyethyl) Disulfide (1.09 g (1.4 eq, 7 mM) and 1,2,3,4,6-peracetylated mannose (4 g, 1 eq, 10.2 mM) in dry dichloromethane (20 mL) stirring at 0 °C. The mixture was allowed to warm to room temperature and stirred at room temperature for 24 hrs. Then the reaction mixture was extracted with 30 mL of Ethyl acetate, washed with sat. NaHCO_3 (3×40 mL) and dried over Na_2SO_4 . Then the crude product was purified by column chromatography (Ethyl acetate/Hexane=1:1) to furnish desired Bis(2-hydroxyethyl)

Disulfide, 2,3,4,6-tetraacetate- α -D-mannopyranoside. Yield =70 %, ^1H NMR (400 MHz, CDCl_3): δ (ppm) = 1.89 (s, 6H, COCH_3), 1.95 (s, 6H, COCH_3), 2.01 (s, 6H, COCH_3), 2.06 (s, 6H, COCH_3), 2.76-2.85 (m, 4H, CH_2S), 3.69 (m, 2H, $\text{CH}_a\text{H}_b\text{CH}_2\text{S}$), 3.78 (m, J = 3.9, 6.2 10.2 Hz, 2H, $\text{CH}_a\text{H}_b\text{CH}_2\text{S}$), 3.85 (m, J = 2.3, 5.7, 9.5 Hz, 2H, 5-H), 4.03 (dd, J = 2.3, 12.2 Hz, 2H, 6-Ha), 4.18 (dd, J = 5.7, 12.2 Hz, 2H, 6-Hb), 4.77 (d, J = 1.7 Hz, 2H, 1-H), 5.14 (dd, J = 1.7, 3.2 Hz, 2H, 2-H), 5.17 (dd, 2 H), 5.21 (dd, J = 3.2, 10.0 Hz, 2H, 3-H);

In a round bottom flask Bis(2-hydroxyethyl) Disulfide 2,3,4,6-tetraacetate- α -Dmannopyranoside (0.2 g, 0.37 mM) was dissolved in 50 mL of methanol. To this NH_3 (0.03 g, 0.55 mM) was added and the mixture was stirred at room temperature for 2 h. the reaction mixture was concentrated in vacuum. ^1H NMR (400 MHz, MeOD): 2.84 (m, 4H, CH_2S), 2.94 (m, 4H, $\text{CH}_2\text{CH}_2\text{S}$), 3.54-3.87 (m, 8H), 3.0-4.00 (m, 4H), 4.96 (S, 8H);

Reference:

- [1] Kohli P., Taylor K.K., Harris J.J., Blanchard G.J., Assembly of Covalently-Coupled Disulfide Multilayers on Gold. **Journal of the American Chemical Society**, 120(46), pp. 11962-11968, **1998**.
- [2] Saga Y., Tamiaki H., Facile synthesis of chlorophyll analog possessing a disulfide bond and formation of self-assembled monolayer on gold surface. **Journal of Photochemistry and Photobiology B: Biology**, 73(1), pp. 29-34, **2004**.
- [3] López-Tobar E., Hernández B., Ghomi M., Sanchez-Cortes S., Stability of the Disulfide Bond in Cystine Adsorbed on Silver and Gold Nanoparticles As Evidenced by SERS Data. **The Journal of Physical Chemistry C**, 117(3), pp. 1531-1537, **2013**.
- [4] Zhang L., Zhang Y., Hu Y., Fan Q., Yang W.J., Li A., Li S., Huang W., Wang L.-H., Refractive index dependent real-time plasmonic nanoprobe on single silver nanocube for ultrasensitive detection of the lung cancer-associated miRNAs. **Chemical Communications**, 51(2), pp. 294-297, **2015**.
- [5] Zhang L., Zhang J., Wang F., Shen J., Zhang Y., Wu L., Lu X., Wang L., Fan Q., Huang W., An Au@Ag nanocube based plasmonic nano-sensor for rapid detection of sulfide ions with high sensitivity. **RSC Advances**, 8(11), pp. 5792-5796, **2018**.
- [6] Zhang Y., Shuai Z., Zhou H., Liu B., Zhang Y., Zhang L., Chen S., Chao J., Weng L., Fan Q., Fan C., Huang W., Wang L., Single-molecule analysis of microRNA and logic operations using a smart plasmonic nanobiosensor. **Journal of the American Chemical Society**, 140(11), pp. 3988-3993, **2018**.